

INTERNATIONAL SOCIETY FOR SOIL MECHANICS AND GEOTECHNICAL ENGINEERING



This paper was downloaded from the Online Library of the International Society for Soil Mechanics and Geotechnical Engineering (ISSMGE). The library is available here:

<https://www.issmge.org/publications/online-library>

This is an open-access database that archives thousands of papers published under the Auspices of the ISSMGE and maintained by the Innovation and Development Committee of ISSMGE.

Construction simulation for the interaction between shield segments and ground

H.Zhu & W.Ding

Department of Geotechnical Engineering, Tongji University, Shanghai, People's Republic of China

T.Hashimoto & J.Nagaya

Geo Research Institute, Osaka Soil Test Laboratory, Japan

T.Tamura

Department of Transportation Engineering, Kyoto University, Japan

ABSTRACT: To simulate the construction process for the interaction between shield segments and ground, the plane strain elasto-plastic construction FEM including Goodman joint model and curved beam-joint element is used. We also pay a great attention to the effects of the gap closing, the grouting pressure distribution and grouting material hardening on the internal forces of structure at the shield tail point. By using variable releasing coefficients that can be obtained from the measured displacements, the different construction sequences of the shield tunneling are simulated continuously. Finally a case study-No.7 subway line in Osaka is analyzed to evaluate the settlement comparing with the measured one and the influences of different contact parameters on the earth pressure and internal forces of structure.

1 INTRODUCTION

The surrounding ground's deformations caused by the excavation of subway, sewage tunnel etc., using shield driving become smaller recently. There are two major reasons: one is due to the new shield methods, such as the earth pressure balancing (EPB) shield and the slurry shield; another belongs to the development of the grouting technique and the grouting material of plasticity. In the mean time, it is shown from the field measurement that the deformations due to shield tail and the time-dependent effect take most parts while the deformations due to the face excavation is a little. So the improvement of the grouting technique and the grouting material as well as the effect of the ground consolidation must be considered.

The ground deformation around the shield tunnel and the external pressure on the lining mostly depends on the grouting technique and the interaction between lining and ground. In the following, by use of the construction 2D-FEM, we will simulate the different construction sequences of the shield tunneling continuously with variable releasing coefficients which can be obtained from the measured displacements, and will compare the settlement of ground with the measured ones.

2 MATERIAL MODEL

2.1 Ground elasto-plastic model and joint model

The ground material is simulated by plane strain

elasto-plastic model that uses Drucker-Prager yield criterion and associated flow rule.

The contact face between the ground and the structure has the special properties; it can transfer not only the normal stress σ_n but also the shear stress τ_s . To simulate this characteristic the contact element is introduced by using Goodman joint model.

When the normal force σ_n is in a compression state, the yielding criterion of the contact element is commonly satisfied with Mohr-Coulomb function.

For non-linear relation between the force with the deformation of contact element, there are

$$\tau_s = K_s \cdot \Delta v \quad \sigma_n = K_n v_m \frac{\Delta u_n}{v_m - \Delta u_n} \quad (\Delta u_n < v_m) \quad (1)$$

Where v_m is the maximum allowable normal embedment value of the contact element.

In this case, the incremental iterated method is chosen to solve the related problems.

2.2 Curved beam-joint model

The lining structure of shield tunnel is assembled by several segment pieces with linking bolts. So in numerical calculation, the segment piece is discretized by several beam elements, and the joint between two segment pieces is modeled by a joint element including a double-node, which is shown in Figure 1. The stiffness of the curved beam element sees reference [2]; the stiffness of joint element can be obtained easily.

$$[K_J] = [A]^T [K] [A] \quad (2)$$

In which $[K_J]$ is the stiffness of the joint element in local coordinates which should be transferred to the global stiffness in the global coordinates, $[K]$ is the stiffness of the joint which is relative to K_n , K_s , K_ϑ , and $[A]$ is a correlative matrix.

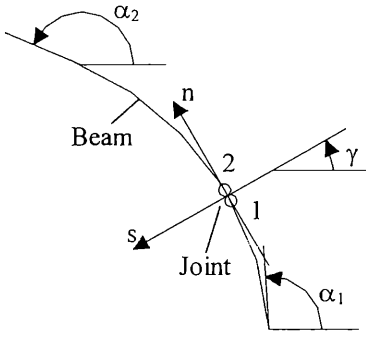


Figure 1. Curved beam-joint model.

Additionally, we know that this model is applicable to elastic bodies which follows a non-linear force-displacement relationship. A nonlinear relation of the rotational stiffness coefficient of the segment joint that depends on the relative rotation $\Delta\vartheta$ is given

$$k_\vartheta = (k_{\vartheta_1} - k_{\vartheta_2}) \cdot e^{-\lambda\Delta\vartheta} + k_{\vartheta_2} \quad (3)$$

In which k_{ϑ_1} , k_{ϑ_2} , λ are the constants obtained from the bending test of the segment joint.

3. SIMULATION OF THE CONSTRUCTION PROCESS OF SHIELD TUNNEL

3.1 Calculation of initial earth stress $\{\sigma_0\}$

1. FEM formation

If using FEM to calculate the initial earth stress $\{\sigma_0\}$ we can obtain it by solving the following equation

$$[K]\{\delta\} = \{F_b\} + \{F_s\} + \{F_c\} \quad (4)$$

$$\{\sigma_0\}^e = [D][B]\{\delta\}^e + \{\sigma_t\} \quad (5)$$

Where $[K]$ is the global stiffness matrix of ground material, $\{\delta\}$ is the global nodal displacement vector, $\{\sigma_t\}$ is tectonic stress which only exists in rock ground, and is often assumed as constant or linear stresses, and $\{F_b\}$, $\{F_s\}$, $\{F_c\}$ are the equivalent

nodal forces of the body forces $\{b\}$ including the dry and wet gravity of soil, the surface loads $\{P\}$ and the concentrated load $\{Q\}$.

2. Lateral pressure formation

In soil ground, the initial stresses can be calculated by FEM or by experimental lateral pressure coefficient K_0 that is generally given as follows

$$K_0 = \begin{cases} 1 - \sin \varphi & \text{for sandy layer} \\ OCR^{0.3} - 0.5 & \text{for clay layer} \end{cases} \quad (6)$$

Where φ is the effective internal friction angle and OCR is the over-consolidation ratio.

3.2 Construction process of shield tunneling and 2-D FEM simulation

3.2.1 Construction process of shield tunneling

As to the construction process in shield tunneling, generally the following four typical stages shown in Figure 2 are usually divided into:

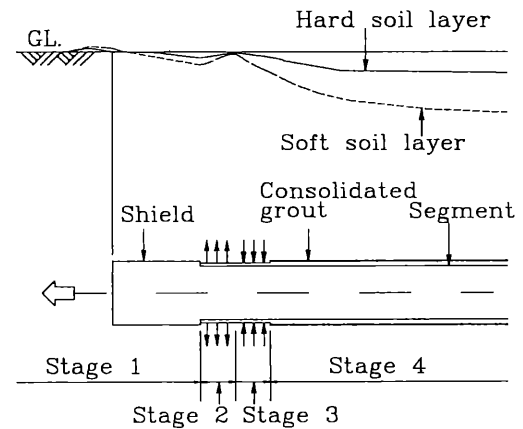


Figure 2. Diagram of the construction process of shield tunneling.

(1) The first is the stage in cutting face and along the length of shield machine.

A balance between the soil pressure before the cutting face and the supporting pressure after the cutting face such as the jacking force, the liquid pressure in slurry shield chamber, the earth pressure in EPB shield and the friction between shield machine and soil ground should be kept.

Along the shield machine, the earth stress of the surrounding soil ground can't release due to the rigid supporting, but the disturbance to the surrounding soil ground caused by the friction between the shield machine and the soil ground with advancing must be

considered. For the slurry shield, according to the measured deformations, the deformation will not occur in hard ground because the slurry ring around tunnel easily forms, and will occur slightly in soft soil ground.

(2) The second is the stage during grouting at the tail point of shield machine.

With shield machine driving, before the shield tail detaches, a special grouting material must be put into the clearance occupied by the cover of shield machine, and the amount of the grouting material is 1.2-1.3 times of the clearance volume. For slurry shield, in hard ground, the internal pressure at the tail is dependent on the slurry pressure, which is greater than the grouting pressure; but in soft ground, it is dependent on the grouting pressure. For earth pressure shield, the internal pressure at the tail is equal to the grouting pressure.

The grouting pressure is also related with the strength of segment pieces, the type of shield machine as well as the characteristic of grouting material. From present construction examples the grouting pressure is within the scope of 0.2-0.4MPa.

(3) The third is the stage of the closure of the clearance between soil ground and lining, in which the settlements of ground occur greatly.

The settlement occurred at this stage depends on the grouting technique such as the synchronous grouting, the semi-synchronous grouting, the instantaneous grouting and the rear grouting. The selection of the grouting technique is relative with the ground condition, the grouting equipment, the requirement to the cross-section of tunnel and the structural type of the shield tail etc.

(4) The final is the stage of the interaction between ground and lining due to hardening of the grouting material and the consolidation of soil.

In one side, the settlement of ground will be restrained gradually and the external loads will transfer to the lining substantially as the grouting material hardens; in another side, the deformation of ground also increases with time due to the soil consolidation. Therefore, the external loads, such as the soil and water pressure and the grouting pressure, can transfer to the lining structure most of which apply on it with the grouting material hardening. So it is necessary to study the grouting material hardening and the grouting pressure distribution to evaluate the mechanical behavior of the lining .

3.2.2 Continuous simulation of construction process using 2-D FEM technique

As to the above four construction processes, a continuous simulation approach different from the past one is adopted in the two dimensional problem. To realize the continuous simulation, the different releasing coefficients of the initial earth stress

(called as IESRC below), that is obtained from the experiences and the measured deformation in the field, is employed to reflect the variations of the construction process at different stage.

In the first stage IESRC is taken as 0.0-0.1. In the second the lining segment is set and the grouting pressure is applied on the contact element between the soil ground and the structure. Together with considering the great heave resulting from the grouting pressure and the earth stress releasing. Consequently, IESEC depends on the magnitude of grouting pressure. In the third, the stress releasing is mainly caused by the clearance of the shield tail, so IESRC value is relative with the clearance volume. In the final, the residual IESRC should be applied.

By using the 2-D FEM technique, the state variation of the above construction process can be described as the following:

$$([K_0] + [\Delta K_i])\{\Delta \delta_i\} = \{\Delta F_{ir}\} + \{\Delta F_{ia}\} \quad (i=1, L) \quad (7)$$

Where L is the number of construction stage, here $L=4$, $[K_0]$ is the initial stiffness matrix of soil and structure (if it exists) before construction, $[\Delta K_i]$ is the increment/decrement of soil and structure stiffness during construction, such as the stiffness of excavated soil element or newly adding/subtracting structure element, $\{\Delta F_{ir}\}$ is the vector of releasing equivalent forces along the excavated boundary, which is determined by the initial stress at first and by the current stress state later, $\{\Delta F_{ia}\}$ is the vector of the newly adding equivalent forces during construction, $\{\Delta \delta_i\}$ is the vector of the incremental nodal displacement at any construction stage.

For the nonlinear elastic model and elasto-plastic model of soil and contact face at any stage, the incremental-iterated technique with constant stiffness within each loading step is used and the concrete calculation equation is expressed as follows

$$[K_{i0}]\{\Delta \delta_i^{jk}\} = \{\Delta F_i^{jk}\} \quad (i=1, L; j=1, M; k=1, N) \quad (8)$$

$$\{\delta_i\} = \sum_{\ell=1}^i \sum_{j=1}^M \{\Delta \delta_\ell^j\} \quad (i=1, L; j=1, M) \quad (9)$$

$$\{\sigma_i\} = \{\sigma_0\} + \sum_{\ell=1}^i \sum_{j=1}^M \{\Delta \sigma_\ell^j\}$$

In which M, N is the number of loading and iterative step respectively, $\{\Delta F_i^{jk}\} = \sum_e \int_{V_e} \{B\}^T \{\Delta \sigma_i^j\} dv$, σ_0 is the initial stresses, and $\{\Delta \sigma_i^j\}$ is the increment of the nonlinear stresses, $\{B\}$ is the strain matrix.

4 CASE STUDY

4.1 Project's outline and geological conditions

The No.7 subway line in Osaka consists of the east bound line that is 970.415m long and the west bound line that is 974.481m long, the depth of overburden is about 16~30m, and the reinforced concrete segment is 1.2m wide and 280mm thick, its outer diameter is 5.300m. Two $\phi 5.440$ m EPB shield machines with synchronous grouting technique construct it.

There are seven soil layers composed of sand and clay alternatively, sees in Figure 3, the Standard Penetration Test (SPT) value varies from 0 to 50. The ground water level is -3m. The shield tunnel lies in AS2 sand layer at the measuring section B.

4.2 Selection of parameters

1. Ground Parameters

The employed ground parameters of cross-section B are in Table 1, for sandy ground, $E=a+bN$, $\varphi=15+\sqrt{15N}$, $K_0=1-\sin\varphi'$, in which φ' is an effective friction angle. For clay ground, $E=bq_u$, $K_0=OCR^{0.3}-0.5$, $C=q_u/2$, in which $q_u=N/50$ (kN/m²).

2. Structure parameters

The parameters of the lining structure are provided usually in designing, for segment we have

Table 1. The employed ground parameters.

Layer	H _i (m)	E (kPa)	μ	φ (°)	C (kPa)	γ_t (kN/m ³)	K ₀
Ac1	2.0	8500	0.43	0	25	-16.0	0.75
Ac2	5.5	20,774	0.43	0	61.1	-16.7	0.75
As1	3.0	39,500	0.35	37.6	0	-16.6	0.55
As2	11.0	49,003	0.35	40.4	0	-16.5	0.55
Ac3	5.0	40,120	0.43	0	118	-17.0	0.75
As3	7.0	48,572	0.35	40.3	0	-16.5	0.55
Ac4	26.0	46,920	0.43	10.	138	-17.4	0.75

$E=3.5\times 10^7$ kN/m², $A=0.28$ m², $I=1.83\times 10^{-3}$ m⁴, and for joint between the segments we have $K_\theta=2.5\times 10^8$ kN·m/m², $K_s=6.55\times 10^7$ kN/m³, $K_n=2.5\times 10^7$ kN/m³.

3. Contact parameters and grouting pressure distribution

The contact element parameters are changeable according to the loading step number. The contact parameters are listed in Table 2.

In table 2, v_m is the maximum allowable embedment value of contact element. In construction stage No.2, the grouting material is in liquid state, and the liquid itself is incompressible, but the contained air void can be compressed, assuming there is 15% air void, then the relation between the grouting pressure and volumetric strain is

$$\varepsilon_v = 0.15 \times \left[1 - \left(\frac{P_a}{P_a + P_g} \right) \right] \quad (10)$$

Where P_a and P_g are atmospheric pressure and the grouting pressure respectively, and $P_a=0.1$ MPa, $P_g=0.15$ MPa. Then K_n can be obtained by

$$K_n = \frac{P_g}{\varepsilon_v \cdot t} \quad (11)$$

Where t is the thickness of shield tail void, and $t=0.07$ m. And considering the flowability of grouting material in this stage, K_s is near to zero.

In construction stage No.3 and No.4, the grouting material has been solidified, and

$$K_s = \frac{K_n}{2(1+\nu)} = \frac{K_n}{2(1+0.3)}. K_n \text{ can be obtained by}$$

$$K_n = \frac{E}{t} = \frac{300C}{t} \quad (12)$$

Where C is cohesion, and $C = \frac{q_u}{2}$. In stage No.3,

$q_u=0.1\sim 0.3$ MPa, in stage No.4, $q_u=1\sim 4$ MPa, in FEM calculation assuming $q_u=0.2$ and 3MPa in stage No.3 and No.4 respectively.

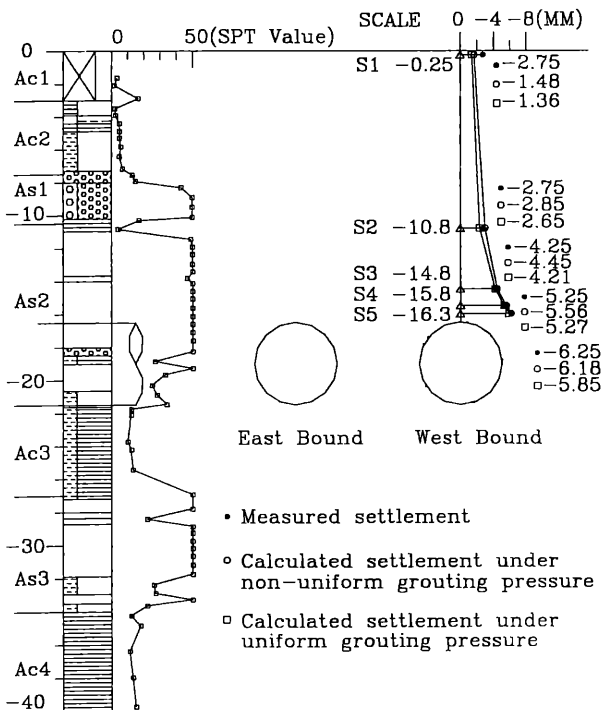


Figure 3. The soil layers of B section and the measured/calculated settlements above the tunnel.

Table 2. The employed contact face's parameters.

Loading step	Shear stiff. K_s (kN/m)	Normal stiff. K_n (kN/m)	φ ($^\circ$)	C (kPa)	v_m (m)
No.1	-	-	-	-	-
No.2	100	2.381×10^4	0.0	0.0	0.02
No.3	1.648×10^5	4.286×10^5	20.0	100.0	0.02
No.4	2.473×10^6	6.429×10^6	50.0	3000.0	0.02

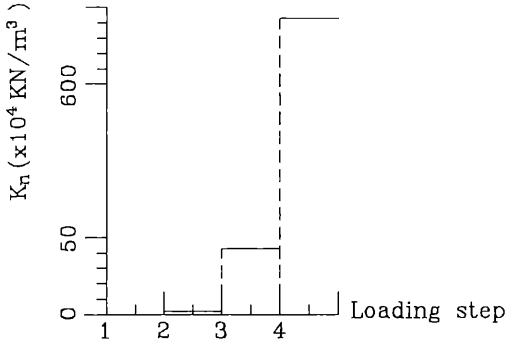


Figure 4. The normal stiffness K_n of the contact element versus the loading step.

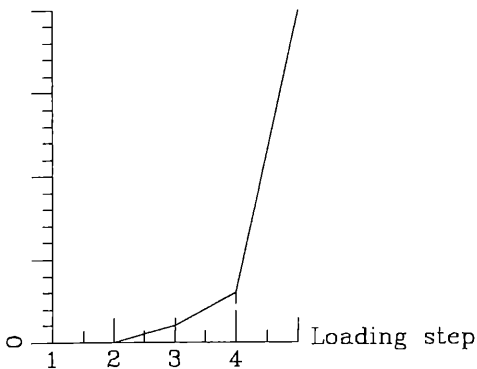
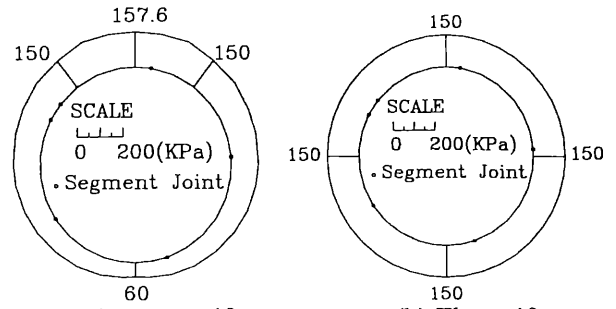


Figure 5. The maximum normal stress σ_n of the contact element versus the loading step.

The relations between the normal stiffness K_n , the maximum normal stress σ_n of contact element and the loading step are demonstrated in Figures 4-5.

The grouting pressure is applied on the segment and the internal border of ground in the second stage (loading step No.2), and there are two kinds of the grouting pressure distribution: the non-uniform and the uniform given according to the site investigation. Under the condition of the non-uniform grouting pressure, if there is one grouting hole, the grouting pressure distribution, which has the included angle θ with x-direction is as follows:

$$P(\theta) = P_1 + P_2 \cos \frac{\theta - \beta}{2} \quad (-\pi \leq \theta - \beta \leq \pi) \quad (13)$$



(a) The non-uniform (b) The uniform
Figure 6. The distribution of the grouting pressure .

Where β is the included angle of the grouting hole and x-direction, and P_1 is the constant pressure as $\theta - \beta$ is equal to zero and P_2 is the constant pressure as $\theta - \beta$ is equal to π ; if there are two grouting holes, which are symmetric to z-axis, the grouting pressure distribution is as follows:

$$P(\theta) = 2P_1 + P_2 \sum_{i=1}^2 \cos \frac{\theta - \beta_i}{2} \quad (-\pi \leq \theta - \beta_1, \theta - \beta_2 \leq \pi) \quad (14)$$

Where β_1, β_2 are the included angles of the grouting hole and x-direction, and $P_1=5.47\text{kPa}$, $P_2=77.32\text{kPa}$, $\beta_2=\pi-\beta_1$, which is demonstrated in Figure 6(a).

The another condition is uniform grouting pressure, which is shown in Figure 6(b).

4. Releasing coefficients of excavation

The releasing coefficients of excavation corresponding with the above four stages are given according to the measured data in the field, there are 0.10, 0.45, 0.3, 0.15 respectively.

4.3 Calculation results of displacements and stresses

The calculated displacements in soil ground around tunnel are shown in Figure 7, the Figure 7(a) are the calculated under the non-uniform grouting pressure and the Figure 7(b) are the calculated under the uniform grouting pressure. With comparison of the two results, the grouting pressure distribution affects the displacements around tunnel, and the displacements at the invert and crown points under the non-uniform condition are greater than those under the uniform condition, the contrary trend is suitable for the displacements at the two horizontal points.

4.4 Comparisons of the calculated results with measured data

The measured/calculated settlements in ground are shown as Table 3. The measured/ calculated settlements in ground are shown in Figure 3.

In order to evaluate any differences between the calculated and the measured, we give the relative

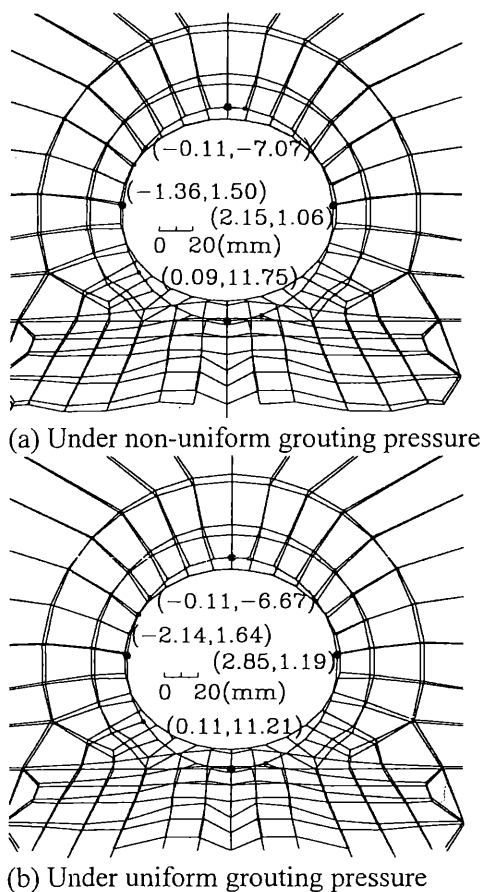


Figure 7. The displaced mesh in loading step No.4

Table 3. The measured/calculated settlements in ground (mm)

Final stage	S1	S2	S3	S4	S5
Measured	-2.75	-2.75	-4.25	-5.25	-6.25
Calculated A	-1.48	-2.85	-4.45	-5.56	-6.18
Calculated B	-1.36	-2.65	-4.21	-5.27	-5.85

Notes: A and B are the calculated values under non-uniform and uniform grouting pressure respectively.

errors of the absolute sum between them for the settlement based on Table 3 in loading step No.4 (the final step). The relative error with the non-uniform grouting pressures is 3.44%, but the relative error with the uniform grouting pressures is 8.99%. We find by comparison that the form of the grouting pressure distribution has a great effect on the calculated results and the calculated under the non-uniform is close to the measured.

5 CONCLUSIONS

In this paper, we use 2-D FEM to simulate the whole construction process in shield driving continuously, and use the Goodman joint element to model the contact face between lining segment and ground, the

curved-beam element to model the segment joint. we also pay a great attention to examining the effects of the gap closing, the grouting pressure distribution and hardening on the displacements in ground and the internal forces of structure at the shield tail point. The following conclusions are obtained:

1. The grouting material hardens gradually with the process of the shield construction, which is simulated through changing the parameters of the grouting material such as the stiffness, the internal friction angle and cohesion at different construction stage.

2. In the study there are two conditions of the grouting pressure: the non-uniform and the uniform distribution. The distribution of the grouting pressure greatly affects the calculated results, such as the displacements around tunnel and the settlements in ground. The calculated results under the non-uniform condition are closer to the corresponding measured data than those under the uniform condition.

3. There is no yielding area around the tunnel and no clear difference under the above two conditions of grouting pressure.

6 REFERENCE

- Akin, J.E. 1982. *Application and implementation of finite element methods*, Academic Press, (in English).
- Zhu H. et al. 1994. Two kinds of design model for joint of segment and lining in shield tunnel, *Engineering Mechanics*, Supplement, pp.395-399, (in Chinese).
- Hashimoto T. et al. 1996. Geotechnical aspects of ground movement during shield tunneling in Japan, *One-day seminar geotechnical aspect of underground structure*, Himpunan Ahliteknik Tanah Indonesia (hatti), Jakarta, pp.1/III-6/III, (in Indonesia).